

# Non-hermitian off-diagonal magnetic response of Dirac fermions

Roberta Zsófia Kiss,<sup>1</sup> Doru Sticlet,<sup>2</sup> Cătălin Pașcu Moca,<sup>3,4</sup> and Balázs Dóra<sup>1,5,\*</sup>

<sup>1</sup>*Department of Theoretical Physics, Institute of Physics,*

*Budapest University of Technology and Economics, Műegyetem rkp. 3., H-1111 Budapest, Hungary*

<sup>2</sup>*National Institute for R&D of Isotopic and Molecular Technologies, 67-103 Donat, 400293 Cluj-Napoca, Romania*

<sup>3</sup>*MTA-BME Quantum Dynamics and Correlations Research Group, Institute of Physics, Budapest University of Technology and Economics, Műegyetem rkp. 3., H-1111 Budapest, Hungary*

<sup>4</sup>*Department of Physics, University of Oradea, 410087, Oradea, Romania*

<sup>5</sup>*MTA-BME Lendület Topology and Correlation Research Group, Budapest University of Technology and Economics, Műegyetem rkp. 3., H-1111 Budapest, Hungary*

(Dated: September 28, 2022)

We perform a comparative study for the magnetization dynamics within linear response theory of one and two dimensional massive Dirac electrons, after switching on either a real (hermitian) or an imaginary (non-hermitian) magnetic field. While hermitian dc magnetic fields polarize the spins in the direction of the external magnetic field, non-hermitian magnetic fields induce only off diagonal response. An imaginary dc magnetic field perpendicular to the mass term induces finite magnetization in the third direction only according to the right hand rule. This can be understood by analyzing the non-hermitian equation of motion of the spin, which becomes analogous to a classical particle in crossed electric and magnetic fields. Therein, the spin expectation value, the mass term and imaginary magnetic field play the role of the classical momentum, magnetic and electric field, respectively. The latter two create a drift velocity perpendicular to them, which gives rise to the off-diagonal component of the dc spin susceptibility, similarly to how the Hall effect develops in the classical description.

## I. INTRODUCTION

With the advent of graphene and topological insulators[1, 2], the Dirac equation has been essentially rediscovered in condensed matter physics, giving rise the plethora of interesting effects in various dimensions and under several conditions. Due to the (pseudo)-spin structure in the Dirac equation[3], a variety of peculiar phenomena such as the anomalous quantum Hall effect, electron chirality and Klein paradox has been observed and this degree of freedom has been suggested to be useful for possible applications in spintronics[4] and pseudospintronics[5].

In order for the (pseudo)-spin structure of the Dirac equation to be useful for applications, one needs to be able to control it with external field. While much is known about this within hermitian quantum mechanics, the effect of non-hermitian external perturbations has been largely unexplored. Non-hermitian systems have been extensively investigated[6–14] and present many unusual features, such as unidirectional invisibility[15], exceptional points[16], supersonic modes[17], the non-hermitian linear response theory[18–20] reveals unexpected features. These include measuring the anticommutators of observables instead of commutators, thus opening the door to access novel physical quantities experimentally as well as containing additional terms due to non-unitary dynamics of non-hermitian systems.

In order to shed light and investigate non-hermitian spin dynamics, we focus on the gapped hermitian Dirac

equation in various dimensions and evaluate the real part of the magnetic susceptibility when the system is perturbed with a hermitian or a non-hermitian external magnetic field. We find that in response to the hermitian magnetic fields, the spin susceptibility is a diagonal tensor in the zero frequency limit, indicating that the induced magnetization always develops in the direction of the applied external field. On the other hand, for imaginary magnetic field, the response is anisotropic and only the  $xy$  component of the real part of the susceptibility is finite in the dc limit for a mass term in the  $z$  direction. This can be understood by mapping the dynamics of the spins onto the classical Newton equation of a particle moving in a Lorentz force from magnetic field and an electric field. The former originates from the mass term while the latter stems from the non-hermitian magnetic field. Within the context of the classical Newton equation, these fields induce a drift velocity perpendicular to them and give rise to a finite momentum for the classical motion, which in turn is responsible for the development of the Hall effect. In our case, in complete *analogy* to the classical scenario, a finite spin component is induced perpendicular to the mass term and imaginary magnetic field, according to the right hand rule.

## II. ONE DIMENSIONAL DIRAC EQUATION

We start with the one dimensional massive Dirac equation, whose Hamiltonian is

$$H_0 = vp\sigma_x + \Delta\sigma_z, \quad (1)$$

\* dora.balazs@ttk.bme.hu

where  $\sigma$ 's are Pauli matrices, denoting the (pseudo-)spin of the particles,  $v$  is the Fermi velocity and  $\Delta$  is the mass term, which couples to  $\sigma_z$ . This is readily diagonalized to yield the spectrum  $E_{\pm} = \pm\sqrt{(pv)^2 + \Delta^2}$ .

We perform a comparative analysis and study the induced magnetization of the system in the long time limit. The system is initially prepared in the ground state of  $H_0$  at half filling with all  $E_-$  energies occupied. At  $t = 0$  the system is perturbed with a weak real (hermitian) or imaginary (non-hermitian) external magnetic field. To this end, we evaluate the *real* part of the frequency dependent susceptibility using the Kubo formula from hermitian and non-hermitian linear response theory, whose dc,  $\omega \rightarrow 0$  limit is responsible for the value of the magnetization in the long time limit.

Let us also note that the particle current operator for the one dimensional Dirac equation is  $v\sigma_x$ , therefore through measuring the magnetic response in the  $x$  direction, implicitly the current correlation function is probed through the magnetoelectric effect[2]. However, for the other direction,  $\sigma_y$  or  $\sigma_z$  cannot be identified as a particle current operator. Nevertheless, all three Pauli matrices can be coupled to by magnetic fields.

### A. Hermitian magnetic field

The magnetic response is evaluated using the Kubo formula for the spin susceptibility

$$\chi_{ij}(t, t') = -i\Theta(\tau)\langle[\sigma_i(\tau), \sigma_j]\rangle_0 \quad (2)$$

in response to an external perturbation of the form  $B\sigma_j$ . Here, the expectation value is taken with respect to the ground state wavefunction of  $H_0$ , and  $[A, B]$  denotes the commutator. Here we introduced  $\tau = t - t'$  and  $\sigma(\tau) = e^{iH_0\tau}\sigma e^{-iH_0\tau}$ . Then, the time dependence of the magnetization follows from

$$\langle\sigma_i(t)\rangle = \int_0^t \chi_{ij}(t, t')B(t')dt'. \quad (3)$$

Using the fact that the susceptibility is time translational invariant,  $\chi_{ij}(t, t') = \chi_{ij}(t - t')$ , and performing the Fourier transformation, we get

$$\langle\sigma_i(\omega)\rangle = \chi_{ij}(\omega)B(\omega). \quad (4)$$

Since our focus is mostly on the possible finite magnetization in the long time limit, we need to evaluate  $\text{Re}\chi(\omega \rightarrow 0)$ , whose non-vanishing value would signal finite magnetic response to a static magnetic field. Using Appendix B, the dc,  $\omega \rightarrow 0$  limit of the real part of the magnetic susceptibilities are

$$\underline{\chi}(0) = \frac{1}{\pi v} \begin{pmatrix} |\text{sgn}(\Delta)| & 0 & 0 \\ 0 & \ln \frac{2W}{|\Delta|} & 0 \\ 0 & 0 & \ln \frac{2W}{|\Delta|} \end{pmatrix}, \quad (5)$$

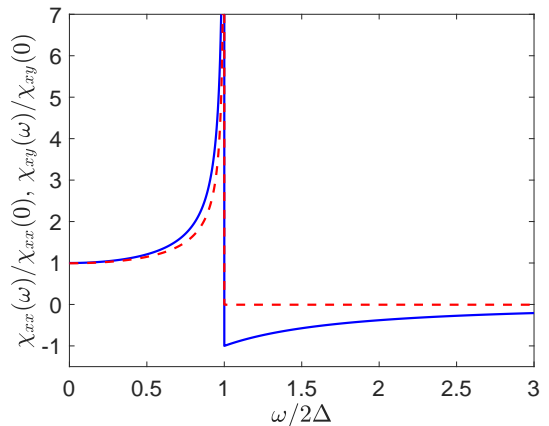


FIG. 1. The real part of the hermitian susceptibility (blue solid line),  $\chi_{xx}$  and the non-hermitian one (red dashed line),  $\chi_{xy}$  is visualized for the one dimensional Dirac equation.

which is a diagonal matrix and  $W$  represents the high energy cutoff. This implies that a constant magnetization in the long time limit develops only in the direction of the applied external magnetic field.

### B. Non-hermitian magnetic field

In the case of imaginary magnetic field, the full problem becomes non-hermitian and the weak perturbation is  $iB\sigma_j$  which is apparently non-hermitian due to the  $i$  prefactor. The magnetic field is applied along the  $j = x, y$  or  $z$ , directions and  $B$  is assumed real and denotes the strength of the non-hermitian magnetic field. Then, the operator to which the external perturbation couples to becomes non-hermitian as  $i\sigma_j$ . The corresponding real part of the susceptibility can be obtained from the non-hermitian Kubo formula[18–20] and Eq. (4) still applies for the non-hermitian setting. In particular, in Ref. 19, some of the authors worked out the non-hermitian linear response theory and applied it to a non-hermitian system (i.e. tachyons) in the presence of hermitian perturbation (vector potential). In contrast to that, we now focus on hermitian systems, namely the Dirac equation, in the presence of a non-hermitian perturbation, an imaginary magnetic field.

Adapting this to the present case of hermitian initial system in non-hermitian, imaginary perturbation, we obtain

$$\chi_{ij}(t, t') = -\Theta(\tau) (\langle\{\sigma_i(\tau), \sigma_j\}\rangle_0 - 2\langle\sigma_i\rangle_0\langle\sigma_j\rangle_0), \quad (6)$$

where  $\{A, B\}$  denotes the anticommutator, which arises instead of the commutator due to the non-hermitian operator  $i\sigma_j$ , which the external field couples to. After some straightforward algebra (see Appendix A) and performing the Fourier transformation to frequency space, the momentum integrals of the non-zero elements for the

real parts are evaluated as

$$\begin{aligned}\chi_{xx}(\omega) &= -\frac{\Delta^2}{2} \int dp \frac{1}{E^2} \delta(2E - |\omega|) = \\ &= -\frac{|\Delta|}{\sqrt{\frac{\omega^2}{4\Delta^2} - 1} |\omega| v} \Theta(\omega^2 - 4\Delta^2),\end{aligned}\quad (7)$$

$$\begin{aligned}\chi_{xy}(\omega) &= \frac{2\Delta}{\pi} \int dp \frac{1}{4E^2 - \omega^2} = \\ &= \frac{\text{sgn}(\Delta)}{2v} \frac{\Theta(4\Delta^2 - \omega^2)}{\sqrt{1 - (\frac{\omega}{2\Delta})^2}},\end{aligned}\quad (8)$$

$$\begin{aligned}\chi_{yy}(\omega) &= -\frac{1}{2} \int dp \delta(2E - |\omega|) = \\ &= -\frac{1}{2\sqrt{1 - \frac{4\Delta^2}{\omega^2}} v} \Theta(\omega^2 - 4\Delta^2),\end{aligned}\quad (9)$$

and

$$\begin{aligned}\chi_{zz}(\omega) &= -\frac{1}{2} \int_{-\infty}^{\infty} dp \frac{(vp)^2}{E^2} \delta(2E - |\omega|) = \\ &= -\frac{1}{2v} \sqrt{1 - \frac{4\Delta^2}{\omega^2}} \Theta(\omega^2 - 4\Delta^2).\end{aligned}\quad (10)$$

The only component which does not exhibit gapped behaviour is  $\chi_{xy}$ , whose frequency dependence is plotted in Fig. 1. The dc limit of the real part of these susceptibilities is evaluated as

$$\underline{\underline{\chi}}(0) = \frac{\text{sgn}(\Delta)}{2v} \begin{pmatrix} 0 & 1 & 0 \\ -1 & 0 & 0 \\ 0 & 0 & 0 \end{pmatrix},\quad (11)$$

which is an off-diagonal matrix, and the only finite elements follows the "right hand rule", namely that the induced magnetization in the long time limit is perpendicular to both the mass term ( $z$  direction in the present case) and the direction of the applied imaginary magnetic field. This is explained in Sec. V.

### III. TWO DIMENSIONAL DIRAC EQUATION

The two dimensional gapped Dirac equation is written as

$$H_0 = v_x p_x \sigma_x + v_y p_y \sigma_y + \Delta \sigma_z, \quad (12)$$

whose spectrum is  $E_{\pm} = \pm \sqrt{(v_x p_x)^2 + (v_y p_y)^2 + \Delta^2}$ , and the system is initially prepared in its ground state at half filling, i.e. the  $E_-$  energies are occupied. Similarly to the one dimensional case, the particle current operators in the  $x$  and  $y$  directions are  $v_x \sigma_x$  and  $v_y \sigma_y$ , while  $\sigma_z$  cannot be identified as a current.

### A. Hermitian magnetic field

We use the conventional Kubo formula again from Eq. (2) and the Appendices. Eventually, in the  $\omega \rightarrow 0$  limit, we get

$$\underline{\underline{\chi}}(0) = \frac{W}{4\pi v_x v_y} \begin{pmatrix} 1 & 0 & 0 \\ 0 & 1 & 0 \\ 0 & 0 & 2 \end{pmatrix}, \quad (13)$$

which is again a diagonal matrix, similarly to the one dimensional case.

### B. Non-hermitian magnetic field

Similarly to the one dimensional case, we use the non-hermitian Kubo formula in Eq. (6). The finite elements of the real part of the frequency dependent susceptibility from the Appendix are

$$\begin{aligned}\chi_{xx}(\omega) &= -\frac{1}{4\pi} \int d^2p \frac{(v_y p_y)^2 + \Delta^2}{E^2} \delta(2E - |\omega|) = \\ &= -\frac{|\omega|}{16v_x v_y} \left( 1 + \frac{4\Delta^2}{\omega^2} \right) \Theta(\omega^2 - 4\Delta^2),\end{aligned}\quad (14)$$

$$\begin{aligned}\chi_{xy}(\omega) &= \frac{\Delta}{\pi^2} \int d^2p \frac{1}{4E^2 - \omega^2} = \\ &= \frac{\Delta}{4\pi v_x v_y} \text{Re} \left( \ln \left( \frac{(W/\Delta)^2}{1 - (\frac{\omega}{2\Delta})^2} + 1 \right) \right),\end{aligned}\quad (15)$$

$\chi_{yy}(\omega) = \chi_{xx}(\omega)$  and

$$\begin{aligned}\chi_{zz}(\omega) &= -\frac{1}{4\pi} \int d^2p \frac{(v_x p_x)^2 + (v_y p_y)^2}{E^2} \delta(2E - |\omega|) = \\ &= -\frac{|\omega|}{8v_x v_y} \left( 1 - \frac{4\Delta^2}{\omega^2} \right) \Theta(\omega^2 - 4\Delta^2).\end{aligned}\quad (16)$$

While the diagonal components are gapped, the only non-vanishing off-diagonal element,  $\chi_{xy}$  is cutoff dependent, which is expected to dominate over the additional frequency dependence. This is shown in Fig. 2.

After taking the  $\omega \rightarrow 0$  limit, we find that the real part of the magnetic susceptibility is off-diagonal, similarly to the one dimensional case as

$$\underline{\underline{\chi}}(0) = \frac{\Delta}{2\pi v_x v_y} \ln \left( \frac{W}{|\Delta|} \right) \begin{pmatrix} 0 & 1 & 0 \\ -1 & 0 & 0 \\ 0 & 0 & 0 \end{pmatrix}. \quad (17)$$

The ensuing structure of Eq. (17) is explained in Sec. V.

### IV. THREE DIMENSIONAL DIRAC-WEYL EQUATION

The three dimensional Dirac-Weyl equation is written as

$$H_0 = v_x p_x \sigma_x + v_y p_y \sigma_y + v_z p_z \sigma_z, \quad (18)$$

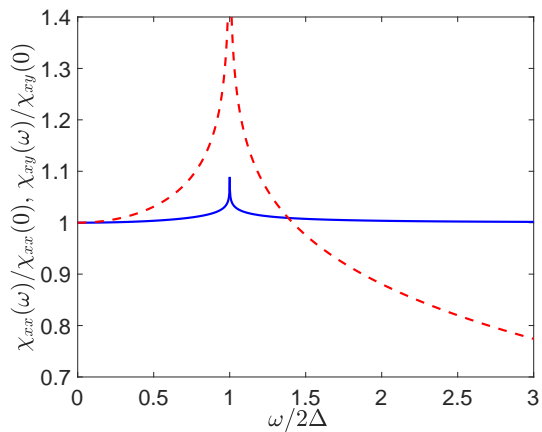


FIG. 2. The real part of the hermitian susceptibility (blue solid line),  $\chi_{xx}$  and the non-hermitian one (red dashed line),  $\chi_{xy}$  is visualized for the two dimensional Dirac equation with  $W/\Delta = 100$ .

whose spectrum is  $E_{\pm} = \pm\sqrt{(v_x p_x)^2 + (v_y p_y)^2 + (v_z p_z)^2}$ . This equation cannot be gapped out, a term of the form  $\Delta\sigma_z$  does not open a gap in the spectrum.

In order to calculate the corresponding susceptibilities, we realize that the three dimensional Dirac-Weyl equation in Eq. (18) can be obtained from the two dimensional gapped Dirac equation from Eq. (12) by replacing  $\Delta$  with  $v_z p_z$ . Consequently, the frequency dependent susceptibility of the former is obtained from that of the latter in Eqs. (A3) and (A4) after the same  $\Delta \rightarrow v_z p_z$  replacement and integrating over  $p_z$ . When moving to the dc limit, the corresponding dc susceptibility is obtained by performing the same replacement in Eqs. (13) and (17). For the hermitian case, the dc susceptibility is finite and independent from  $\Delta$  in Eq. (13) for the two dimensional case. By moving to the Dirac-Weyl case with the  $\Delta \rightarrow v_z p_z$  replacement and integrating over  $p_z$ , the dc limit of the hermitian susceptibility is finite as  $\chi(0) \sim W^2$ , as already identified for three dimensional Dirac semimetals in Ref. 21.

In contrast, Eq. (17) is odd in  $\Delta$  for the non-hermitian case in two dimensions. Due to this, by moving into the Dirac-Weyl case with  $\Delta \rightarrow v_z p_z$  change and momentum integration, it will vanish. Therefore, we find that the dc limit of the non-hermitian susceptibilities for Dirac-Weyl systems are zero as

$$\chi(0) = 0. \quad (19)$$

No finite magnetization can be induced by a static, imaginary magnetic field at half filling (when the  $E_-$  band is filled).

By applying the same procedure to Eqs. (14), (15) and (16), we obtain the frequency dependent non-hermitian susceptibilities as well. The off-diagonal components vanish (Eq. (15) is odd in  $\Delta$ ) and the diagonals are equals to each other as  $\chi(\omega) = -\omega^2/24\pi v_x v_y v_z$ .

## V. EQUATION OF MOTION FOR THE SPIN

The off-diagonal nature of the real part of the non-hermitian dc magnetic susceptibility can be understood by inspecting the equation of motion for the spins[22]. We consider the full non-hermitian Hamiltonian with  $H = (\mathbf{A}_{\mathbf{p}} + i\mathbf{B}) \cdot \boldsymbol{\sigma}$ , where  $\mathbf{A}_{\mathbf{p}} = (vp, 0, \Delta)$  for the one dimensional case and  $\mathbf{A}_{\mathbf{p}} = (v_x p_x, v_y p_y, \Delta)$  for the two dimensional case and  $i\mathbf{B}$  denotes the imaginary time independent magnetic field, that is switched on at  $t = 0$ . The expectation value of the spin for a given momentum is evaluated from[12, 23–25]

$$\langle \boldsymbol{\sigma}_{\mathbf{p}}(t) \rangle = \frac{\langle \Psi_{\mathbf{p}} | e^{iH^+ t} \boldsymbol{\sigma} e^{-iHt} | \Psi_{\mathbf{p}} \rangle}{\langle \Psi_{\mathbf{p}} | e^{iH^+ t} e^{-iHt} | \Psi_{\mathbf{p}} \rangle}, \quad (20)$$

and the system starts from lowest energy eigenstate,  $\Psi_{\mathbf{p}}$ , of  $\mathbf{A}_{\mathbf{p}} \cdot \boldsymbol{\sigma}$ . The equation of motion for the spin for a given momentum  $\mathbf{p}$  reads as

$$\partial_t \langle \boldsymbol{\sigma}_{\mathbf{p}}(t) \rangle = 2\mathbf{A}_{\mathbf{p}} \times \langle \boldsymbol{\sigma}_{\mathbf{p}}(t) \rangle - 2\mathbf{B} + 2\langle \boldsymbol{\sigma}_{\mathbf{p}}(t) \rangle [ \langle \boldsymbol{\sigma}_{\mathbf{p}}(t) \rangle \cdot \mathbf{B} ], \quad (21)$$

which resembles closely to the Newton's equation of a classical particle in a crossed electric and magnetic field. Here,  $\langle \boldsymbol{\sigma}_{\mathbf{p}}(t) \rangle$  represents the classical momentum,  $\mathbf{A}_{\mathbf{p}}$  plays the role of the magnetic field and the first term on the r.h.s. of Eq. (21) represents the Lorentz force,  $\mathbf{B}$  represents an electric field and the last term is the relativistic correction.

In a crossed electric and magnetic field, the particle experiences a drift velocity for the guiding center[26], which is perpendicular to both the electric and magnetic field. In this case, this effective "drift velocity" points towards  $\mathbf{B} \times \mathbf{A}_{\mathbf{p}}$ , and after averaging over momentum, in order to get the total spin as  $\sum_{\mathbf{p}} \langle \boldsymbol{\sigma}_{\mathbf{p}}(t) \rangle$ , it becomes perpendicular to both the  $z$  direction (the direction of the mass term, which does not average out) and the direction of the imaginary magnetic field. This results in an effective magnetization in the perpendicular direction, in agreement with Eqs. (11) and (17), similarly to how the Hall-effect develops in the classical case.

The equation of motion method also allows us to analyze the three dimensional Dirac-Weyl case with  $\mathbf{A}_{\mathbf{p}} = (v_x p_x, v_y p_y, v_z p_z)$ , which can be obtained from the two dimensional case after the  $\Delta \rightarrow v_z p_z$  change and integration over  $p_z$ , similarly to Sec. IV. For a given fix  $p_z$ , there will be a finite magnetization developing perpendicular to both the non-hermitian magnetic field and  $z$  direction, analogously to the two dimensional case. However, this will be compensated exactly by the contribution of the  $-p_z$  term, which arises from the momentum integration. This will cancel the magnetization from the  $+p_z$  term and yield Eq. (19).

## VI. EXPERIMENTAL POSSIBILITIES

In terms of experimental realization, various forms of the Dirac equation in various spatial dimensions have al-

ready been realized[1, 27–32] both in condensed matter and cold atomic systems as well as in photonic crystals. In an open quantum system, interacting with its environment, the non-hermitian term (i.e. the imaginary magnetic field) arises from an effective Lindblad equation without the recycling term[23, 24] through continuous monitoring of the system and postselection[23, 24], using jump operators for bonds[17, 33, 34]. This results in the appropriate imaginary magnetic fields for the one, two and three dimensional Dirac equations. By preparing the system in a given initial state with the  $E_-$  band filled and coupling it weakly to environment, the (pseudo-)magnetization in a given direction can be measured, which would directly yield the calculated susceptibilities.

One can also profit from the recent non-hermitian realization of spin-orbit coupled fermions[35]. By considering weak spin dependent  $^{173}\text{Yb}$  atom losses, a non-hermitian magnetic field can be engineered. By monitoring the ensuing time dependent spin profile, the non-hermitian spin susceptibility is directly accessible after Fourier transformation to frequency space.

Photonic waveguides[8, 31, 32, 36] are also used to emulate the non-hermitian Dirac equation, with the complex refractive index due to losses representing the non-hermitian term. Weak imaginary magnetic fields are created by weak losses, and by measuring light propagation across the experimental setup yields the non-hermitian pseudo-magnetic susceptibilities within the validity range of our linear response calculations.

Additionally, single photon interferometry is also available to realize Dirac equation in the presence of non-hermitian magnetic fields[37] directly in momentum space. By preparing the system in the lower energy band and controlling the time evolution in the presence of weak non-hermitian terms by a variety of optical elements, the time dependent magnetization can be obtained.

## VII. CONCLUSIONS

We studied the magnetization dynamics in terms of the real part of the frequency dependent spin susceptibility of one, two and three dimensional gapped Dirac electrons, in response to hermitian or non-hermitian magnetic fields. By focusing on the long time limit of the magnetization, we find that a hermitian magnetic field induces diagonal response and the ensuing spin expectation value points in the direction of the external perturbation. In sharp contrast, a non-hermitian magnetic field triggers off-diagonal response according to the right hand rule: a constant magnetization develops in the direction perpendicular to both the direction of the mass term and that of the non-hermitian magnetic field. This is understood by mapping the equation of motion of the spin to a Newton equation of a classical particle in electric and magnetic fields, the latter giving rise to the Lorentz force. In the classical case, a finite drift velocity develops perpendicular to both the electric and magnetic fields. Analogously for the spin, a finite spin expectation value is only expected perpendicular to both the mass term and the imaginary magnetic field. Our results could be useful for further manipulation of the spin of Dirac particles in open quantum systems and in dissipative environment.

## ACKNOWLEDGMENTS

Useful discussions with Ferenc Simon, János Asbóth are gratefully acknowledged. This research is supported by the National Research, Development and Innovation Office - NKFIH within the Quantum Technology National Excellence Program (Project No. 2017-1.2.1-NKP-2017-00001), K142179, K134437, by the BME-Nanotechnology FIKP grant (BME FIKP-NAT), and by a grant of the Ministry of Research, Innovation and Digitization, CNCS/CCCDI-UEFISCDI, under Projects No. PN-III-P4-ID-PCE-2020-0277 and PN-III-P1-1.1-TE-2019-0423.

- 
- [1] A. H. Castro Neto, F. Guinea, N. M. R. Peres, K. S. Novoselov, and A. K. Geim, *The electronic properties of graphene*, Rev. Mod. Phys. **81**, 109 (2009).
- [2] M. Z. Hasan and C. L. Kane, *Colloquium: Topological insulators*, Rev. Mod. Phys. **82**, 3045 (2010).
- [3] D. Song, V. Paltoglou, S. Liu, Y. Zhu, D. Gallardo, L. Tang, J. Xu, M. Ablowitz, N. K. Efremidis, and Z. Chen, *Unveiling pseudospin and angular momentum in photonic graphene*, Nature Communications **6**, 6272 (2015).
- [4] M. He, H. Sun, and Q. L. He, *Topological insulator: Spintronics and quantum computations*, Front. Phys. **14**, 43401 (2019).
- [5] D. P. and Allan H. MacDonald, *Spintronics and pseudospintronics in graphene and topological insulators*, Nature Materials **11**, 409 (2012).
- [6] T. Gao, E. Estrecho, K. Y. Bliokh, T. C. H. Liew, M. D. Fraser, S. Brodbeck, M. Kamp, C. Schneider, S. Höfling, Y. Yamamoto, F. Nori, Y. S. Kivshar, *et al.*, *Observation of non-hermitian degeneracies in a chaotic exciton-polariton billiard*, Nature **526**, 554 (2015).
- [7] I. Rotter and J. P. Bird, *A review of progress in the physics of open quantum systems: theory and experiment*, Rep. Prog. Phys. **78**, 114001 (2015).
- [8] J. M. Zeuner, M. C. Rechtsman, Y. Plotnik, Y. Lumer, S. Nolte, M. S. Rudner, M. Segev, and A. Szameit, *Observation of a topological transition in the bulk of a non-hermitian system*, Phys. Rev. Lett. **115**, 040402 (2015).
- [9] L. Feng, Z. J. Wong, R.-M. Ma, Y. Wang, and X. Zhang, *Single-mode laser by parity-time symmetry breaking*, Sci-

- ence **346**(6212), 972 (2014).
- [10] H. Hodaei, A. U. Hassan, S. Wittek, H. Garcia-Gracia, R. El-Ganainy, D. N. Christodoulides, and M. Khajavikhan, *Enhanced sensitivity at higher-order exceptional points*, Nature **548**, 187 (2017).
- [11] E. J. Bergholtz, J. C. Budich, and F. K. Kunst, *Exceptional topology of non-hermitian systems*, Rev. Mod. Phys. **93**, 015005 (2021).
- [12] Y. Ashida, Z. Gong, and M. Ueda, *Non-hermitian physics*, Advances in Physics **69**, 3 (2020).
- [13] R. El-Ganainy, K. G. Makris, M. Khajavikhan, Z. H. Musslimani, S. Rotter, and D. N. Christodoulides, *Non-hermitian physics and  $pt$  symmetry*, Nat. Phys. **14**(1), 11 (2018).
- [14] M. Fruchart, R. Hanai, P. B. Littlewood, and V. Vitelli, *Non-reciprocal phase transitions*, Nature **592**, 363 (2021).
- [15] Z. Lin, H. Ramezani, T. Eichelkraut, T. Kottos, H. Cao, and D. N. Christodoulides, *Unidirectional invisibility induced by  $PT$ -symmetric periodic structures*, Phys. Rev. Lett. **106**, 213901 (2011).
- [16] W. D. Heiss, *The physics of exceptional points*, J. Phys. A: Math. Theor. **45**(44), 444016 (2012).
- [17] Y. Ashida and M. Ueda, *Full-counting many-particle dynamics: Nonlocal and chiral propagation of correlations*, Phys. Rev. Lett. **120**, 185301 (2018).
- [18] L. Pan, X. Chen, Y. Chen, and H. Zhai, *Non-hermitian linear response theory*, Nature Physics **16**, 767 (2020).
- [19] D. Sticlet, B. Dóra, and C. P. Moca, *Kubo formula for non-hermitian systems and tachyon optical conductivity*, Phys. Rev. Lett. **128**, 016802 (2022).
- [20] K. T. Geier and P. Hauke, *From non-hermitian linear response to dynamical correlations and fluctuation-dissipation relations in quantum many-body systems*, PRX Quantum **3**, 030308 (2022).
- [21] Y. Ominato and K. Nomura, *Spin susceptibility of three-dimensional dirac-weyl semimetals*, Phys. Rev. B **97**, 245207 (2018).
- [22] R. Botet and H. Kuratsuji, *The duality between a non-hermitian two-state quantum system and a massless charged particle*, Journal of Physics A: Mathematical and Theoretical **52**(3), 035303 (2018).
- [23] A. J. Daley, *Quantum trajectories and open many-body quantum systems*, Advances in Physics **63**, 77 (2014).
- [24] H. Carmichael, *An Open Systems Approach to Quantum Optics* (Springer-Verlag, Berlin, 1993).
- [25] E. M. Graefe, H. J. Korsch, and A. E. Niederle, *Mean-field dynamics of a non-hermitian bose-hubbard dimer*, Phys. Rev. Lett. **101**, 150408 (2008).
- [26] T. G. Northrop, *The guiding center approximation to charged particle motion*, Annals of Physics **15**(1), 79 (1961).
- [27] R. Gerritsma, G. Kirchmair, F. Zähringer, E. Solano, R. Blatt, and C. F. Roos, *Quantum simulation of the dirac equation*, Nature **463**(7277), 68 (2010).
- [28] L. Tarruell, D. Greif, T. Uehlinger, G. Jotzu, and T. Esslinger, *Creating, moving and merging Dirac points with a Fermi gas in a tunable honeycomb lattice*, Nature **483**, 302 (2012).
- [29] L. Lamata, J. León, T. Schätz, and E. Solano, *Dirac equation and quantum relativistic effects in a single trapped ion*, Phys. Rev. Lett. **98**, 253005 (2007).
- [30] T. E. Lee, U. Alvarez-Rodriguez, X.-H. Cheng, L. Lamata, and E. Solano, *Tachyon physics with trapped ions*, Phys. Rev. A **92**, 032129 (2015).
- [31] B. Zhen, C. W. Hsu, Y. Igarashi, L. Lu, I. Kaminer, A. Pick, S.-L. Chua, J. D. Joannopoulos, and M. Soljacic, *Spawning rings of exceptional points out of dirac cones*, Nature **525**, 354 (2015).
- [32] W. Song, S. Gao, H. Li, C. Chen, S. Wu, S. Zhu, and T. Li, *Demonstration of imaginary-mass particles by optical simulation in non-hermitian systems* ArXiv:2011.08496.
- [33] Z. Gong, Y. Ashida, K. Kawabata, K. Takasan, S. Higashikawa, and M. Ueda, *Topological phases of non-hermitian systems*, Phys. Rev. X **8**, 031079 (2018).
- [34] Y. Takasu, T. Yagami, Y. Ashida, R. Hamazaki, Y. Kuno, and Y. Takahashi,  *$PT$ -symmetric non-Hermitian quantum many-body system using ultracold atoms in an optical lattice with controlled dissipation*, Progress of Theoretical and Experimental Physics **2020**(12) (2020), 12A110.
- [35] Z. Ren, D. Liu, E. Zhao, C. He, K. K. Pak, J. Li, and G.-B. Jo, *Chiral control of quantum states in non-hermitian spin-orbit-coupled fermions*, Nat. Phys. **18**, 385 (2022).
- [36] S. Longhi, *Optical realization of relativistic non-hermitian quantum mechanics*, Phys. Rev. Lett. **105**, 013903 (2010).
- [37] L. Xiao, D. Qu, K. Wang, H.-W. Li, J.-Y. Dai, B. Dóra, M. Heyl, R. Moessner, W. Yi, and P. Xue, *Non-hermitian kibble-zurek mechanism with tunable complexity in single-photon interferometry*, PRX Quantum **2**, 020313 (2021).
- [38] T. Giamarchi, *Quantum Physics in One Dimension* (Oxford University Press, Oxford, 2004).
- [39] L. Zhao, H. Deng, I. Korzhovska, Z. Chen, M. Konczykowski, A. Hruban, V. Oganesyanyan, and L. Krusin-Elbaum, *Singular robust room-temperature spin response from topological dirac fermions*, Nature Materials **13**, 580 (2014).
- [40] A. Scholz and J. Schliemann, *Dynamical current-current susceptibility of gapped graphene*, Phys. Rev. B **83**, 235409 (2011).

## Appendix A: Calculation of the susceptibility

In one dimension with hermitian magnetic field, we get

$$\underline{\chi}(t, t') = \frac{1}{2\pi} \int dp \frac{2}{E^2} \begin{pmatrix} \Delta^2 \sin(2E\tau) & \Delta E \cos(2E\tau) & -\Delta v p \sin(2E\tau) \\ -\Delta E \cos(2E\tau) & E^2 \sin(2E\tau) & v p E \cos(2E\tau) \\ -\Delta v p \sin(2E\tau) & -v p E \cos(2E\tau) & (v p)^2 \sin(2E\tau) \end{pmatrix} \Theta(\tau). \quad (\text{A1})$$

where  $E = \sqrt{(v p)^2 + \Delta^2}$ .

In one dimension with imaginary magnetic field, we obtain

$$\underline{\underline{\chi}}(t, t') = \frac{1}{2\pi} \int dp \frac{2}{E^2} \begin{pmatrix} -\Delta^2 \cos(2E\tau) & \Delta E \sin(2E\tau) & \Delta vp \cos(2E\tau) \\ -\Delta E \sin(2E\tau) & -E^2 \cos(2E\tau) & vpE \sin(2E\tau) \\ \Delta vp \cos(2E\tau) & -vpE \sin(2E\tau) & -(vp)^2 \cos(2E\tau) \end{pmatrix} \Theta(\tau). \quad (\text{A2})$$

In two dimensions with hermitian magnetic field, the susceptibility is

$$\begin{aligned} \underline{\underline{\chi}}(t, t') &= \frac{1}{4\pi^2} \int dp_x dp_y \frac{2}{E^2} \begin{pmatrix} ((v_y p_y)^2 + \Delta^2) & -(v_y p_y)(v_x p_x) & -(v_x p_x)\Delta \\ -(v_y p_y)(v_x p_x) & ((v_x p_x)^2 + \Delta^2) & -(v_y p_y)\Delta \\ -(v_x p_x)\Delta & -(v_y p_y)\Delta & ((v_x p_x)^2 + (v_y p_y)^2) \end{pmatrix} \sin(2E\tau)\Theta(\tau) \\ &+ \frac{1}{4\pi^2} \int dp_x dp_y \frac{2}{E} \begin{pmatrix} 0 & \Delta & -(v_y p_y) \\ -\Delta & 0 & (v_x p_x) \\ (v_y p_y) & -(v_x p_x) & 0 \end{pmatrix} \cos(2E\tau)\Theta(\tau), \end{aligned} \quad (\text{A3})$$

where  $E = \pm\sqrt{(v_x p_x)^2 + (v_y p_y)^2 + \Delta^2}$ . The two dimensional case with imaginary magnetic field yields

$$\begin{aligned} \underline{\underline{\chi}}(t, t') &= \frac{1}{4\pi^2} \int dp_x dp_y \frac{2}{E^2} \begin{pmatrix} -((v_y p_y)^2 + \Delta^2) & (v_y p_y)(v_x p_x) & (v_x p_x)\Delta \\ (v_y p_y)(v_x p_x) & -((v_x p_x)^2 + \Delta^2) & (v_y p_y)\Delta \\ (v_x p_x)\Delta & (v_y p_y)\Delta & -((v_x p_x)^2 + (v_y p_y)^2) \end{pmatrix} \cos(2E\tau)\Theta(\tau) \\ &+ \frac{1}{4\pi^2} \int dp_x dp_y \frac{2}{E} \begin{pmatrix} 0 & \Delta & -(v_y p_y) \\ -\Delta & 0 & (v_x p_x) \\ (v_y p_y) & -(v_x p_x) & 0 \end{pmatrix} \sin(2E\tau)\Theta(\tau). \end{aligned} \quad (\text{A4})$$

The susceptibility of three dimensional Dirac-Weyl fermions follows from Eqs. (A3) and (A4) after replacing  $\Delta$  with  $v_z p_z$ .

## Appendix B: Frequency dependent susceptibilities for hermitian magnetic field

### 1. One dimension

Based on Appendix A, the non-vanishing components of the real part of the susceptibility (with  $W$  the high energy cutoff) are

$$\begin{aligned} \chi_{xx}(\omega) &= \frac{2\Delta^2}{\pi} \int dp \frac{1}{E(4E^2 - \omega^2)} = -\frac{1}{\pi v} \frac{1}{|\frac{\omega}{2\Delta}|} \times \\ &\times \text{Re} \left( \frac{1}{\sqrt{(\frac{\omega}{2\Delta})^2 - 1}} \text{atanh} \left( \frac{1}{\sqrt{1 - (\frac{2\Delta}{\omega})^2}} \right) \right) \end{aligned} \quad (\text{B1})$$

with  $E = \sqrt{(vp)^2 + \Delta^2}$  and  $f$  denoting Cauchy's principal value of an integral,

$$\begin{aligned} \chi_{xy}(\omega) &= \frac{\Delta}{2} \int dp \frac{1}{E} \delta(2E - |\omega|) = \\ &= \frac{\Delta}{\sqrt{\omega^2 - 4\Delta^2} v} \Theta(\omega^2 - 4\Delta^2), \end{aligned} \quad (\text{B2})$$

$$\begin{aligned} \chi_{yy}(\omega) &= \frac{2}{\pi} \int dp \frac{E}{4E^2 - \omega^2} = \frac{1}{\pi v} \left( \ln \left( \frac{2W}{|\Delta|} \right) - \right. \\ &\left. - \text{Re} \left( \frac{1}{\sqrt{1 - (\frac{2\Delta}{\omega})^2}} \text{atanh} \left( \frac{1}{\sqrt{1 - (\frac{2\Delta}{\omega})^2}} \right) \right) \right), \end{aligned} \quad (\text{B3})$$

and

$$\begin{aligned} \chi_{zz}(\omega) &= \frac{2}{\pi} \int dp \frac{(vp)^2}{E(4E^2 - \omega^2)} = \frac{1}{\pi v} \left( \ln \left( \frac{2W}{|\Delta|} \right) - \right. \\ &\left. - \text{Re} \left( \sqrt{1 - \left( \frac{2\Delta}{\omega} \right)^2} \text{atanh} \left( \frac{1}{\sqrt{1 - (\frac{2\Delta}{\omega})^2}} \right) \right) \right) \end{aligned} \quad (\text{B4})$$

In the continuum limit, the allowed momenta region is extended to infinity, but in order to make contact with the original model, a cutoff needs to be introduced for certain non-universal physical quantities. The cutoff presence is rather natural in effective low energy theories[38], and accounts for the finite bandwidth, which is present in the original tight binding Hamiltonian, and stems from the finite Brillouin zone.

Among these components,  $\chi_{xy}$  exhibits a gapped behaviour (i.e.  $|\omega| > 2\Delta$  is required), while  $\chi_{yy}$  and  $\chi_{zz}$  are dominated by the cutoff dependent term, which dominates over the additional frequency dependences. The frequency dependence of the cutoff independent  $\chi_{xx}$  is shown in Fig. 1.

## 2. Two dimensions

Based on Appendix A, we get

$$\chi_{xx}(\omega) = \frac{1}{\pi^2} \int d^2p \frac{(v_y p_y)^2 + \Delta^2}{E(4E^2 - \omega^2)} = \frac{(W - |\Delta|)}{4\pi v_x v_y} + \frac{|\omega|}{8\pi v_x v_y} \left( 1 + \left( \frac{2\Delta}{\omega} \right)^2 \right) \text{Re} \left( \text{atanh} \left( \left| \frac{2\Delta}{\omega} \right| \right) \right), \quad (\text{B5})$$

where  $E = \pm \sqrt{(v_x p_x)^2 + (v_y p_y)^2 + \Delta^2}$ ,  $\chi_{yy}(\omega) = \chi_{xx}(\omega)$  and

$$\begin{aligned} \chi_{xy}(\omega) &= \frac{\Delta}{4\pi} \int d^2p \frac{1}{E} \delta(2E - |\omega|) = \\ &= \frac{\Delta}{4v_x v_y} \Theta(\omega^2 - 4\Delta^2), \end{aligned} \quad (\text{B6})$$

and

$$\begin{aligned} \chi_{zz}(\omega) &= \frac{1}{\pi^2} \int d^2p \frac{(v_x p_x)^2 + (v_y p_y)^2}{E(4E^2 - \omega^2)} = \frac{(W - |\Delta|)}{2\pi v_x v_y} + \\ &+ \frac{|\omega|}{4\pi v_x v_y} \left( 1 - \left( \frac{2\Delta}{\omega} \right)^2 \right) \text{Re} \left( \text{atanh} \left( \left| \frac{2\Delta}{\omega} \right| \right) \right). \end{aligned} \quad (\text{B7})$$

The diagonal components scale with the cutoff, which is expected to overwhelm the additional frequency dependences, while the off-diagonal piece,  $\chi_{xy}$  exhibits gapped behaviour and contributes only for  $|\omega| > 2\Delta$ . We note that similar cutoff dependent spin susceptibility,  $\chi(\omega \rightarrow 0) \sim W$ , was observed experimentally for two dimensional topological Dirac fermions[39]. Therein, by measuring the singular spin response of Dirac fermions, the effective cutoff was extracted from the experimental data in Fig. 3 of 39. In addition,  $\chi_{xx}(\omega)$  agrees with the dynamical current-current susceptibility of gapped graphene in Ref. 40.

## 3. Three dimensions

By replacing  $\Delta$  with  $v_z p_z$  in Eq. (A3) and performing the momentum integrals, we find that the resulting susceptibility is diagonal and the diagonal elements are equal as

$$\chi(\omega) = \frac{1}{3\pi^2 v_x v_y v_z} \left( W^2 + \frac{\omega^2}{4} \ln \left( \frac{4W^2 + \omega^2}{\omega^2} \right) \right). \quad (\text{B8})$$

It is dominated by the first, frequency independent term  $\sim W^2$ .